Biometals (2008) 21:93–103
DOI 10.1007/s10534-007-9096-5

Utilization of Fe^{3+}-acinetoferrin analogs as an iron source by *Mycobacterium tuberculosis*

G. Marcela Rodriguez · Richard Gardner · Navneet Kaur · Otto Phanstiel IV

Received: 21 November 2006 / Accepted: 5 March 2007 / Published online: 31 March 2007

Abstract *Mycobacterium tuberculosis*, the causative agent of human tuberculosis, synthesizes and secretes siderophores in order to compete for iron (an essential micronutrient). Successful iron acquisition allows *M. tuberculosis* to survive and proliferate under the iron-deficient conditions encountered in the host. To examine structural determinants important for iron siderophore transport in this pathogen, the citrate-based siderophores petrobactin, acinetoferrin and various acinetoferrin homologs were synthesized and used as iron transport probes. Mutant strains of *M. tuberculosis* deficient in native siderophore synthesis or transport were utilized to better understand the mechanisms involved in iron delivery via the synthetic siderophores. Acinetoferrin and its derivatives, especially those containing a cyclic imide group, were able to deliver iron or gallium into *M. tuberculosis* which promoted or inhibited, respectively, the growth of this pathogen.

Keywords Mycobacterium tuberculosis · Siderophores · Iron · Exosiderophores · Acinetoferrin · Mycobactin

Introduction

Tuberculosis continues to be a public health problem worldwide. The emergence of multi-drug resistant strains of *Mycobacterium tuberculosis* and the association of tuberculosis with AIDS underlines the urgent need for new tools to facilitate the treatment and prevention of this disease (DeAngelis and Flanigan 2005).

Like most living organisms *M. tuberculosis* requires iron as a cofactor of enzymes involved in vital cellular functions. Due to the poor aqueous solubility of ferric ion (Fe^{3+}) in the presence of oxygen and at neutral pH, free iron (III) is not found in the mammalian host, but is sequestered in complexes with iron binding proteins such as transferrin, lactoferrin and ferritin (Weinberg 1984). Therefore, in order to establish a productive infection, *M. tuberculosis* must be able to overcome the iron deficiency imposed by the host. A common mechanism by which bacteria acquire iron is the synthesis and secretion of high-affinity iron chelators (siderophores) that can solubilize iron in the environment

Electronic Supplementary Material The online version of this article (doi:10.1007/s10534-007-9096-5) contains supplementary material, which is available to authorized users.

G. M. Rodriguez (✉)
The Public Health Research Institute at the International Center for Public Health, University of Medicine and Dentistry of New Jersey, 225 Warren Street, Newark, NJ 07103-3535, USA
e-mail: marcela@phri.org

R. Gardner · N. Kaur · O. Phanstiel IV
Department of Chemistry, University of Central Florida, Orlando, FL 32816-2366, USA

and efficiently compete with iron-binding proteins of the host. Specific receptors and membrane transporters are expressed by siderophore producing microorganisms to internalize iron-siderophore complexes (Braun and Killmann 1999). Iron uptake systems are attractive targets for the development of antimicrobial agents that interfere with iron acquisition. In addition, as iron uptake is essential for the pathogen, iron transport systems could be exploited to deliver antibiotics into the bacterial cell in the form of siderophore–antibiotic conjugates (Girijavallabhan and Miller 2004; Roosenberg et al. 2000) This is highly desirable in the case of mycobacteria, which have an exceptionally lipid-rich cell wall. The cell wall provides both a permeability barrier and imparts natural resistance to several antibiotics (Jarlier and Nikaido 1994). Thus, a clear understanding of the molecular mechanisms involved in iron acquisition in *M. tuberculosis* may open new possibilities to combat this pathogen.

When faced with iron limitation, *M. tuberculosis*, produces mycobactins **1** and carboxymycobactins also called exomycobactins **2** (Fig. 1). These siderophores share a common core structure composed of a 2-hydroxyphenyl-oxazoline moiety, a β-hydroxy carbonyl motif and two N^{ϵ}-(hydroxy) lysine residues (Gobin et al. 1995). They differ in the length of the alkyl substitution at R_1 (see Fig. 1). A long alkyl chain (e.g., 10–21 carbons) is found in mycobactins, whereas a shorter one (2–9 carbons) is found in carboxymycobactins (Ratledge and Dover 2000). Mycobactin derivatives containing very short R_1 groups (e.g., CH_3) have been found to be ineffective due to their low lipid solubility (Xu and Miller 1998). Both the carboxymycobactins and mycobactins are not single molecules, but rather a suite of

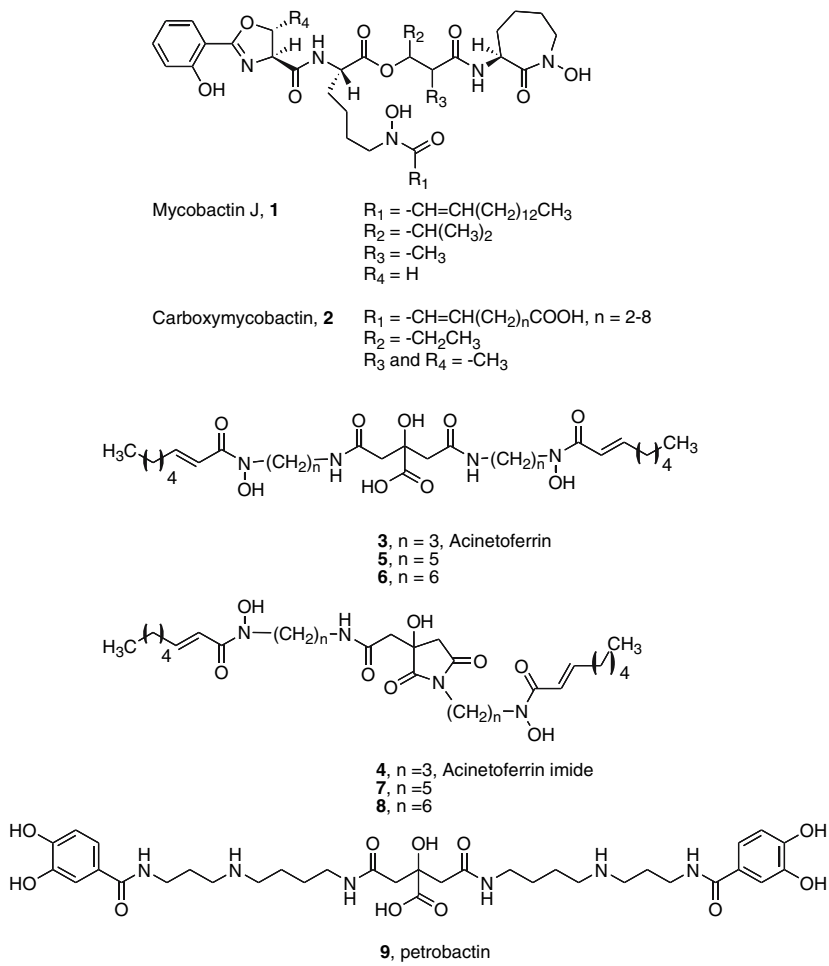

Fig. 1 Structures of iron chelators

siderophores that vary in the number of carbon atoms in the fatty-acid tail. A cluster of 10 genes (*mbtA* to *mbtJ*) encode the enzymes for mycobactin and carboxymycobactin core synthesis. Inactivation of the *mbtB* gene in *M. tuberculosis* prevents production of both mycobactin and carboxymycobactin confirming a common pathway for the synthesis of these two siderophores (De Voss et al. 2000). Carboxymycobactins are one of the few amphiphilic siderophores among the hundreds that have been structurally characterized. Other amphiphilic siderophores include corrugatin, produced by *Pseudomona corrugata*; ornibactins, produced by *Pseudomona cepacia*; rhizobactin, produced by *Sinorhizobium melioti*; amphibactins, produced by *Vibrio* sp. R10 and acinetoferrin, produced by *Acinetobacter haemolyticus* (Budzikiewicz 2004; Winkelmann 1991). Carboxymycobactins are secreted into the medium whereas mycobactin, being a lipophilic siderophore remains associated with the cell membrane (Gobin et al. 1995; Ratledge et al. 1982). After chelating available iron, carboxymycobactin can either transfer iron to mycobactin on the cell surface (Gobin and Horwitz 1996) or it can deliver it into the cell by a process that is independent of mycobactin (Rodriguez and Smith 2006) (Fig. 6). The significance of iron transfer from one siderophore to the other is unclear. Understanding the exact contribution of each siderophore to iron transport in *M. tuberculosis* awaits the isolation of mutants that are defective in the production of one, but not the other siderophore.

The fact that *M. tuberculosis* mutants defective in siderophore synthesis or transport do not survive low iron conditions in vitro and are attenuated for growth in infected macrophages and mice underlines the importance of siderophore-mediated iron acquisition for virulence of this pathogen (De Voss et al. 2000; Rodriguez and Smith 2006). Despite its importance, little is known of the molecular events involved in iron transport in *M. tuberculosis*. IrtAB is an ABC transporter believed to transport Fe^{3+}-carboxymycobactin complexes and, is regulated by iron and the iron-dependent regulator IdeR (Rodriguez et al. 2002). IrtAB is required for efficient utilization of Fe^{3+}-carboxymycobactin, growth in low iron medium and replication in infected macrophages and mice (Rodriguez and Smith 2006). Since inactivation of IrtAB in *M. tuberculosis* does not completely eliminate the ability to survive low iron conditions alternative siderophore transporters must exist. Multiple systems for iron uptake are not uncommon among bacterial pathogens. Several pathogens have parallel pathways for internalizing not only the siderophore(s) synthesized by the organism but also siderophores produced by other bacteria (exosiderophores or xenosiderophores). Studies of xenosiderophore transport have revealed alternative routes for iron acquisition and contribute to the understanding of the molecular mechanisms involved in iron-siderophore transport (Loper and Henkels 1999; Payne and Mey 2004).

Numerous studies of growth promotion and radiolabeled Fe^{3+}-siderophore uptake, conducted with the non-virulent mycobacterium *M. smegmatis*, have shown utilization of various natural and synthetic exosiderophores, some of them involving specific, yet uncharacterized transport systems (Heggemann et al. 2001; Lin et al. 2001; Matzanke et al. 1997; Reissbrodt et al. 1997; Schumann and Mollmann 2001; Wittmann et al. 2004). We have previously demonstrated that the virulent mycobacterium, *M. paratuberculosis*, can utilize acinetoferrin (from *Acinetobacter haemolyticus*) and various synthetic derivatives, especially those containing a cyclic imide motif (Gardner et al. 2004a; Guo et al. 2002). To the best of our knowledge, this is the first study that examines exosiderophore utilization in *M. tuberculosis*. Here, we show that *M. tuberculosis* has the capacity to acquire iron from acinetoferrin and related citrate-based, synthetic siderophores by a low affinity pathway independent of native siderophores and a high affinity pathway that probably involves ligand exchange with mycobactin.

Materials and methods

Reagents

Silica gel (32–63 μm) was purchased from Scientific Adsorbents, Inc. The iron complex of mycobactin J was purchased from Allied Monitor Company in Fayette, MO.

Bacteria, media and growth conditions

Mycobacterium tuberculosis H37Rv was obtained from American Type Culture Collection (ATCC).

The siderophore deficient *mbtB* mutant strain (ST142) (De Voss et al. 2000) was obtained from Dr. Clifton E. Barry III at the National Institute of Allergy and Infectious Disease, Rockville MD. The *irtAB* mutant strain (ST73) was described previously (Rodriguez and Smith 2006). *M. tuberculosis* strains were maintained in Middlebrook 7H9 broth or on 7H10 agar (Difco), supplemented with 0.2% glycerol, 0.05% Tween-80 and 10% albumin–dextrose–NaCl-complex (ADN). *M. tuberculosis* was grown in low iron conditions as previously described (Rodriguez and Smith 2006). Briefly, a defined medium (MM) containing 0.5% w/v asparagine, 0.5% w/v KH_2PO_4, 2% glycerol, 0.5 mg/l 0.05% Tween-80 and 10% ADN was used. The pH was adjusted to 6.8. To lower the trace metal contamination, the medium was treated with Chelex-100 (Bio-Rad Laboratories) according to manufacturer's instructions. Chelex was removed by filtration and before use, the medium was supplemented with 0.5 mg/l $ZnCl_2$, 0.1 mg/l $MnSO_4$, 40 mg/l $MgSO_4$ and the desired concentration of $FeCl_3$.

Synthesis of iron chelators, **3–9**

The respective siderophores have been synthesized previously (Gardner et al. 2004a, b; Guo et al. 2002; Wang and Phanstiel 1998). Details of the synthetic steps involved and their respective structural characterizations have been reported. In general, each siderophore was synthesized by coupling an appropriately protected amine motif to the citric acid core. This was possible by first activating a protected citrate derivative as a bis-*N*-hydroxy ester and coupling it to two equivalents of the respective primary amine. The resultant bis-amides were then deprotected to provide the desired siderophores. The ferric form of the siderophores was prepared by mixing equimolar amounts of the respective siderophore and $FeCl_3$.

Fe^{3+}-Carboxymycobactin purification

Carboxymycobactins were extracted from the culture filtrate of *M. tuberculosis* H37Rv according to the protocol of Gobin et al. (1995). Briefly, H37Rv was grown in a rotator at 37°C in MM supplemented with 2 μM $FeCl_3$ and lacking Tween-80 and ADN for 10 days. The culture supernatant was collected, filtered through a 0.2 μm filter and saturated with iron (III) (0.015%). Fe^{3+}-carboxymycobactins were extracted into chloroform. The chloroform layer was dried overnight with anhydrous $MgSO_4$, filtered through a fritted glass filter and concentrated. The residue was re-suspended in 95% ethanol. The residue was then purified by flash silica gel chromatography using 5% MeOH/$CHCl_3$ as the eluant. Fractions were collected and analyzed by UV absorption on normal-phase silica TLC plates. Fractions containing carboxymycobactins were both UV-active and appeared as red-brown spots on the TLC plate (under visible light). The siderophore-containing fractions were pooled to provide purified carboxymycobactin. LC-MS analysis provided the molecular weights of the carboxymycobactin populations. The average molecular weight was used in terms of molar calculations. The data from the TLC and LC-MS analysis is available in the Supporting Information.

Growth assays

Mycobacterial strains from frozen stocks were inoculated onto 7H10 agar plates. An aliquot was taken from the 7H10 plate to grow a liquid culture in MM with no iron added. Pre-incubation in MM with no iron was done in order to exhaust stored iron. The *mbtB* ST142 was pre-incubated in MM for 24 h (one generation) before incubation with the different Fe^{3+}-siderophores. H37Rv and the *irtAB* mutant (ST73) were grown in MM from an OD of 0.1 to 0.8 (three generations) and then diluted in MM to an OD of 0.1. After 2 days, the cultures were diluted again to an OD of 0.05 in medium containing the different compounds.

Calculation of clogP

Calculated logP (clogP) values were obtained using ChemDraw Ultra 2002, version 7.0.3, purchased from CambridgeSoft in Cambridge, MA.

Relative iron binding affinities of the iron chelators

Relative affinities for iron were obtained based on the rate of change on the absorbance of a Fe^{3+}-chrome azurol S-HDTMA solution (CAS) caused by the

removal of iron by each iron chelator (Schwyn and Neilands 1987). Each siderophore stock solution (4 µl of a 2.4 mM stock) was mixed with 1 µl of EtOH and then added to 95 µl of the CAS solution (150 µM) in a 96-well plate to give a final siderophore concentration of 96 µM. The plate was incubated at 25°C and the decrease in absorbance at 630 nm was measured at regular time intervals in a Thermo max microplate reader (Molecular Devices). The slope of the plot of A(630 nm) versus time (s) was negative as the CAS iron complex was stripped of iron by the respective siderophore.

Results and discussion

Previously, we demonstrated that *M. paratuberculosis* utilized acinetoferrin and its synthetic derivatives. In particular, the imide homolog **4** was superior to mycobactin J compound **1**, in stimulating growth of this mycobacterium. We also found that derivatives containing longer tether lengths between the iron-binding ligands (e.g., **7**) were better stimulators of *M. paratuberculosis* growth (Gardner et al. 2004a). Based on these observations and the fact that both acinetoferrin and carboxymycobactin are amphiphilic siderophores, we decided to test acinetoferrin (**3**), two linear derivatives containing five (e.g., compound **5**) and six (**6**) carbon tethers as well as the acinetoferrin cyclic imide derivatives containing five (e.g., compound **7**) and six (**8**) carbon tethers, for their ability to provide iron to *M. tuberculosis*. In addition, petrobactin, a bis-catecholate containing siderophore (**9**) produced by *Marinobacter hydrocarbonoclasticus* (an oil-degrading bacteria) (Barbeau et al. 2002; Bergeron et al. 2003; Gardner et al. 2004b) and *Bacillus anthracis* (Koppisch et al. 2005) was also evaluated. In this regard, petrobactin **9** represented a non-acinetoferrin-derived citrate based xenosiderophore with different iron binding motifs (catechols in **9** versus hydroxamic acids in **3**–**8**) for comparison (Fig. 1).

To determine whether *M. tuberculosis* utilized the different iron chelators, the siderophore mutant strain (ST142) was used. ST142 does not produce carboxymycobactin or mycobactin, due to inactivation of *mbtB* (De Voss et al. 2000). As a consequence this strain does not grow in low iron conditions, unless carboxymycobactin is provided in the medium (Rodriguez and Smith 2006). Thus, by using this strain one can assess utilization of the synthetic siderophores independently of the native siderophores. For this purpose ST142 was incubated with 10 µM of the different Fe^{3+}-siderophores, respectively, (as described in Materials and methods) and growth was monitored by an increase in optical density (OD). As shown in Fig. 2, acinetoferrin and its derivatives were able to promote the growth of ST142 demonstrating that *M. tuberculosis* is able to utilize the ferric complexes of acinetoferrin and its homologs as an iron source. As previously observed in *M. paratuberculosis*, the acinetoferrin imides **7** and **8** also outperformed the linear systems **5** and **6** in *M. tuberculosis*. In contrast to acinetoferrin and its homologs, petrobactin **9** did not support the growth of ST142 even at a concentration of 100 µM (data not shown). Therefore, not all iron citrate complexes were equally efficient in cross-feeding the mycobacteria indicating, that there is a molecular recognition element involved, which is able to discern between these constructs.

The fact that the linear siderophore, which contains a longer distance (n = 6) (**6**) between the iron-binding motifs provided enhanced growth may be due to either (a) increased hydrophobicity of the siderophore iron complex, (b) stronger iron binding affinity due to the more flexible ligand, (c) ability to adopt a preferred shape for uptake via the iron

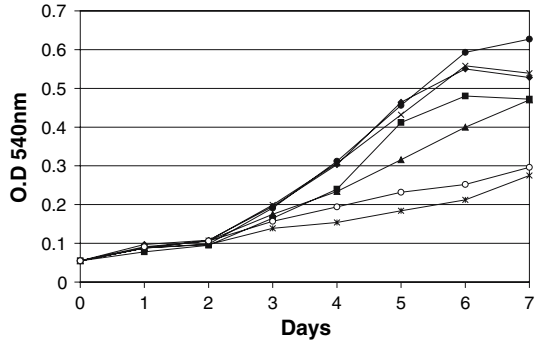

Fig. 2 Growth of the *M. tuberculosis* siderophore mutant strain ST142 in MM (✱) or MM supplemented with 10 µM $FeCl_3$ (○) or the same concentration of each Fe-siderophore complex. Acinetoferrin, Fe^{3+}-**3** (■), Fe^{3+}-**5** (▲), Fe^{3+}-**6** (✖), Fe^{3+}-**7** (♦) and Fe^{3+}-**8** (•). The result of one representative experiment is shown. The experiment was repeated three times

transport system or (d) a combination of these factors. To have an insight into siderophore properties associated with more efficient iron delivery, logP values of compounds **1–9** were calculated (clogP). In general, compounds with high clogP values are considered to be more hydrophobic than those with lower clogP values. As shown in Table 1, there seemed to be a direct correlation between growth index and clogP. Interestingly, siderophores **7** and **8** that were superior growth stimulants have clogP values near 7, which is similar to the clogP estimated for the highest molecular weight carboxymycobactin **2** (clogP: 7.06) but lower than mycobactin (clogP: 10.78). It has been suggested that there might be a significant advantage to bacteria that ''secrete a suite of iron chelators that cover a range of membrane affinities and hydrophobicities'' (Luo et al. 2006). In this regard, it will be interesting to test if differences in hydrophobicity and possibly, membrane affinity of the carboxymycobactins produced by *M. tuberculosis*, correlates with differences in iron capture and/or delivery and whether compounds **7** and **8** mimic the properties of the more efficient forms of carboxymycobactin.

Table 1 clogP, growth index values and rate for iron complexation from CAS

Siderophore	clogP value	Growth index[a]	Slope of curve *A* 630 nm vs. *t*[b]
1	10.78	ND	ND
2	3.89 (n = 2); 7.06 (n = 8)	ND	ND
3	4.25	2.7	−1.39 ± 0.16
4	6.06	ND	ND
5	4.72	1.9	−0.73 ± 0.08
6	5.78	3.4	−0.62 ± 0.07
7	6.71	3.4	−0.56 ± 0.11
8	7.77	3.8	−0.59 ± 0.06
9	−4.16	ND	−1.58 ± 0.01

[a] Growth index (GI) refers to the experiment shown in Fig. 2 and is equal to the optical density, OD, at 540 nm reached by day 6 (×10). The OD of the culture with no iron added was subtracted. Linear regression analysis of a plot of GI versus clogP gave a line with GI = 0.52 (clogP value) and r^2 = 0.66; ND = not determined

[b] The slope and standard deviation (×10,000) of the plots of absorbance at 630 nm (y axis) versus time (s) (t) (x axis) for three independent mixes of each siderophore and Fe^{3+}-CAS

To determine if the iron-binding affinity of compounds **3–9** correlated with iron delivery we estimated the relative affinity of each siderophore based on the rate constant for the formation of the Fe^{3+}-siderophore complex upon removal of iron from the Fe^{3+}-CAS complex. A known concentration of each siderophore was mixed with an excess of Fe^{3+}-CAS and the decrease in absorbance at 630 nm ($A_{630\ nm}$) was measured at regular time intervals against a blank containing no siderophore. The rate constant for the formation of the Fe^{3+}-siderophore complex was calculated as the slope of the linear plot of $A_{630\ nm}$ versus time (t) (s). As shown in Table 1 petrobactin has a high relative affinity than acinetoferrin and its analogs. This observation agrees with previous studies that indicate that cathecol-containing siderophores have a higher affinity for iron than hydroxamate-containing siderophores (Anderegg et al. 1963; Harris et al. 1979). No direct correlation between the ability to promote growth of *M. tuberculosis* and the relative affinity for Fe^{3+} was observed. Petrobactin **9** which exhibited a higher affinity than acinetoferrin **3** and derivatives **5–8** and lower hydrophobicity according to clogP estimates did not support growth of *M. tuberculosis*. In contrast, compounds **7** and **8**, which had moderate iron affinity and higher hydrophobicity were more efficient in supporting growth of ST142. Although other factors like the charge of the compounds and pH sensitivity of the iron complexes may play a role in iron delivery, the results of growth support, clogP values and relative affinities obtained in these experiments suggest that exosiderophores that better interact with the hydrophobic surface of *M. tuberculosis* and more readily release iron, deliver this metal in a more efficient way. Understanding the exact mechanism of iron delivery whether there is active transport of the Fe^{3+}-siderophore complex into the cell or ligand exchange on the bacterial surface will be the focus of future studies.

We next compared the efficiency of iron delivery of the exosiderophores to that of the native siderophores: mycobactin and carboxymycobactin. The ferric complex of mycobactin J, **1**, is available from commercial sources, but carboxymycobactin **2** is not. Therefore, carboxymycobactin was purified from the culture supernatant of *M. tuberculosis*. For this purpose, *M. tuberculosis* was cultured under low iron conditions and carboxymycobactin was extracted

from the culture filtrate as its ferric-complex. The chloroform extract containing Fe^{3+}-carboxymycobactin was purified by column chromatography and the iron-active fractions were analyzed by TLC and LC-MS (available as Supporting Information). Carboxymycobactin **2** technically exists as a series of homologs each differing by a single CH_2 group (with mass differences = 14 g/mol). The average molecular weight was used for the molar dosing of this siderophore.

The activity of the purified carboxymycobactin was tested in growth promotion assays using ST142. As shown in Fig. 3A, purified carboxymycobactin promotes the growth of ST142 at a concentration as low as 10 nM. Comparison of the two natural siderophores demonstrates that carboxymycobactin is a superior iron donor than mycobactin J (Fig. 3A). This is consistent with the fact that carboxymycobactin is secreted in the medium to chelate environmental iron (III) and therefore a pathway to actively transport this siderophore guarantees efficient iron uptake. Mycobactin, however, is not as efficient as carboxymycobactin in delivering iron. Due to its higher hydrophobicity, mycobactin is not normally secreted and is typically associated with the hydrophobic cell wall. Nevertheless, it is interesting that mycobactin J can still deliver iron into the cell, albeit at lower efficiency. The mechanism involved should be addressed in further studies. The most efficient of the synthetic acinetoferrin derivatives, **7** and **8**, required micromolar concentrations to support the growth of ST142 (Fig. 3B). Thus, compared to carboxymycobactin, these siderophores were largely less efficient in delivering iron into *M. tuberculosis.* To determine whether **7** and **8** use the same permease as carboxymycobactin we evaluated utilization of **7** and **8** in strain ST73 in which the genes encoding the ABC transporter IrtAB had been inactivated (Rodriguez and Smith 2006). As shown in Fig. 4 at a concentration as low as 50 nM, Fe^{3+}-**7** and Fe^{3+}-**8** were able to stimulate the growth of ST73 and maximum growth was achieved at 1 μM concentration. As shown in Fig. 3B, 1 μM of Fe^{3+}-**7** and Fe^{3+}-**8** was insufficient to support growth of the ST142 after 4 days of incubation. Thus, **7** and **8** not only were utilized by ST73, but they delivered iron to this strain more efficiently than to ST142. These results indicate that iron delivery by **7** and **8** does not require IrtAB and it is more efficient in the strain deficient in siderophore transport (ST73) than in the strain deficient in siderophore production (ST142).

The difference in the utilization-efficiencies of **7** and **8** in ST142 and ST73 suggest that (a) the lack of natural siderophores synthesis somehow affects the ability to utilize the synthetic siderophores, or (b) xenosiderophore utilization is induced in the irtAB mutant (ST73) perhaps as a compensatory response to the defect in carboxymycobactin utilization. To distinguish between these two possibilities, the relative utilization of **8** by the parental strain H37Rv (which is wild type for siderophore synthesis and transport) and by ST73 was compared.

As shown in Fig. 5, being defective in siderophore transport, ST73 grows poorly in iron-deficient medium compared to the wild type strain. However, addition of 1 μM of Fe^{3+}-**8** complex stimulates the

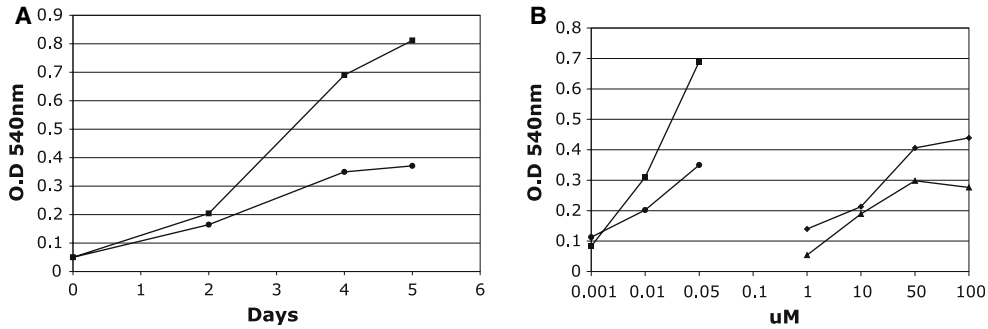

Fig. 3 (**A**) Growth of the *M. tuberculosis* siderophore mutant strain ST142 in the presence of 50 nM of purified Fe^{3+}-carboxymycobactin **2** (■) or Fe^{3+}-mycobactin **1** (•). (**B**) Growth of ST142 after 4 days of incubation in the presence of increasing concentrations of Fe^{3+}-carboxymycobactin **2** (■), Fe^{3+}-mycobactin **1**, (•) Fe^{3+}-**7** (♦) and Fe^{3+}-**8** (▲). The experiment was repeated five times one representative experiment is shown

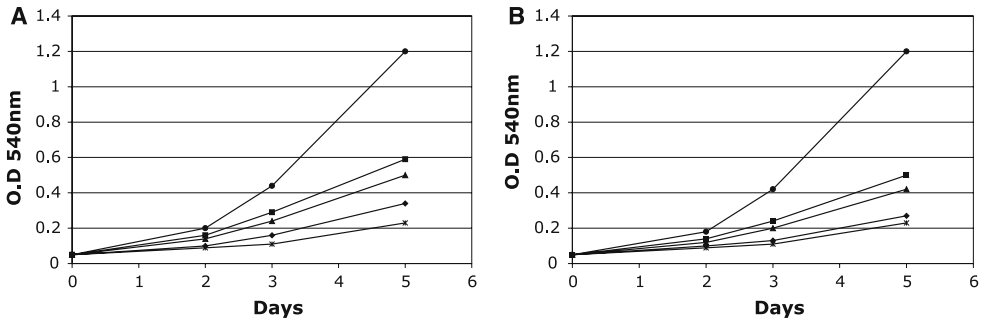

Fig. 4 Growth of the IrtAB mutant strain (ST73) in the presence of increasing concentrations of (**A**) Fe^{3+}-**7** and (**B**) Fe^{3+}-**8**, as iron donors. MM no iron added (*), 10 nM (♦), 50 nM (▲), 100 nM (■), 1 μM (•). The result of one representative experiment is shown. The experiment was repeated three times

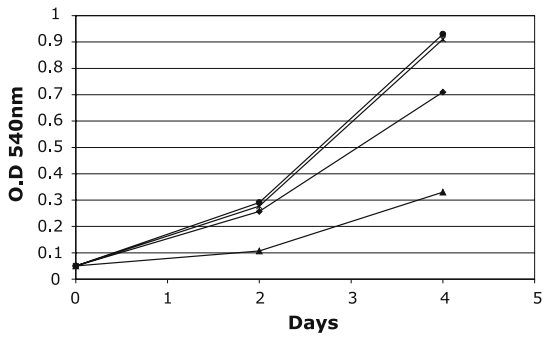

Fig. 5 H37Rv and ST73 were grown in MM and MM supplemented with 1 μM of compound **8**. H37Rv in MM (♦), H37Rv with 1 μM Fe^{3+}-**8** (•), ST73 in MM (▲), ST73 with 1 μM Fe^{3+}-**8** (*). The result of one representative experiment is shown. The experiment was repeated twice

growth of H37Rv and ST73 in a comparable manner. Thus, the efficiency of iron delivery by Fe^{3+}-**8** in the ST73 mutant is similar to that of the wild type strain (Fig. 5). Equivalent results were obtained with Fe^{3+}-**7** (data not shown). This result argues against compensatory induction of an alternative pathway for utilization of the synthetic siderophores in ST73 and supports the idea that ST142 lacks a high affinity pathway for utilization of the synthetic siderophores. The fact that blocked production of the natural siderophores (**1** and **2**) influences the uptake of iron complexes of the synthetic siderophores indicates that efficient delivery of iron by **7** and **8** requires mycobactin and/or carboxymycobactin. The fact that iron delivery via **7** and **8** is not affected by the *irtAB* mutation, suggest that the main route of entry is not as Fe^{3+}-carboxymycobactin. Iron may be transferred from **7** or **8** to carboxymycobactin and then to mycobactin or directly to mycobactin. Differences in iron binding affinities and concentration in the membrane, particularly in the case of mycobactin, may play a role in this iron exchange between siderophores. Upon transfer of iron to mycobactin in the membrane this siderophore can by itself mediate iron entry or alternatively, it may be necessary for the proper functioning of a membrane translocator that recognizes iron complexed to **7** and **8**.

Taken together, the results of growth support assays in the different strains indicate that there are at least two ways by which **7** and **8** can be utilized by *M. tuberculosis*: (a) A low affinity pathway that is independent of carboxymycobactin or mycobactin revealed in the siderophore mutant strain (ST142) (Fig. 6 path A) which may involve internalization of the Fe^{3+}-siderophore complex or transfer of iron to a

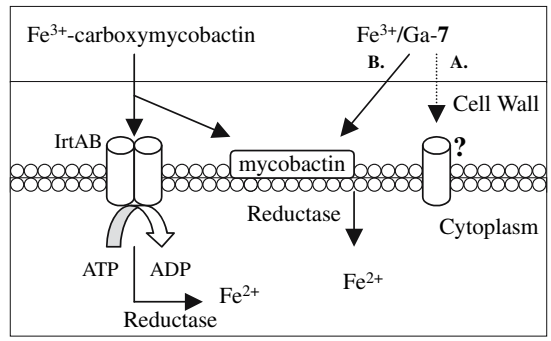

Fig. 6 Iron-siderophore transport in *M. tuberculosis*. The native sideropore carboxymycobactin uses the ABC transporter IrtAB to deliver iron into the cell or it transfers iron to mycobactin on the cell surface. Release of iron from mycobactin probably involves a reductase. Similarly, the synthetic acinetoferrin derivative **7** can deliver iron by a low affinity pathway that is independent of mycobactin (A) or by a higher affinity pathway that depends on mycobactin (B)

metal transporter and, (b) a high affinity pathway which takes place in siderophore producing strains (ST73 and H37Rv) and therefore it is likely to involve ligand exchange to the native siderophores (most likely to mycobactin) (Fig. 6 path B). Indeed, this pathway was not affected by a mutation in the carboxymycobactin transporter IrtAB suggesting that transfer of the metal to carboxymycobactin and delivery through a carboxymycobactin transport pathway independent of mycobactin does not occur. The amphiphilic nature of acinetoferrin and its derivatives probably confers to these molecules the capacity to mimic carboxymycobactins and to access mycobactin on the membrane. Subsequently, transfer of iron to mycobactin facilitates iron uptake (Fig. 6).

Since the synthetic siderophores were generated as metal-free ligands (Gardner et al. 2004a), we were able to also generate complexes with other metal ions. To better evaluate the contribution of the cyclic acinetoferrin derivative **7** to metal ion uptake the gallium complex of **7** was generated. Since gallium is toxic to mycobacteria, this new toxic complex provided the opportunity to relate siderophore delivery to a cytotoxic response. Gallium [as $Ga(NO_3)_3$] has been shown to compete with iron for uptake into *M. tuberculosis* and is toxic to this bacterium probably because it can substitute for Fe^{3+} and disrupt many cellular processes (Olakanmi et al. 2000). Indeed, gallium and iron complexes have been shown to have very similar structures and both bind to hydroxy carboxylic acid ligands (Hawkes et al. 2001; Matzapetakis et al. 1998).

The synthetic derivative **7** was allowed to bind Ga (III) and the growth of *M. tuberculosis* wild type H37Rv and the ST73 strain was measured in a low iron medium in the absence of Ga and in the presence of $[Ga(NO_3)_3]$ or the Ga^{3+}-7 complex. Figure 7 shows the percentage of growth of H37Rv and ST73 in medium containing $[Ga(NO_3)_3]$ or Ga^{3+}-7 in relation to the growth in medium containing no Ga. As previously observed, $[Ga(NO_3)_3]$ reduced the growth of mycobacteria, but the toxicity of Ga was higher, when it was added as the Ga^{3+}-**7** complex. Growth of both H37Rv and ST73 was reduced about 50% in the presence of Ga^{3+}-**7** compared to the growth obtained in the presence of $Ga(NO_3)_3$ (Fig. 7). This result indicates that enhanced delivery of the toxic gallium ions via the complex with **7** resulted in enhanced toxicity to the mycobacteria. Moreover, it demonstrates that in the presence of the native siderophores, the synthetic siderophore-**7** can access the iron- uptake machinery and has the capacity to deliver either Fe or Ga into the cell (Fig. 6).

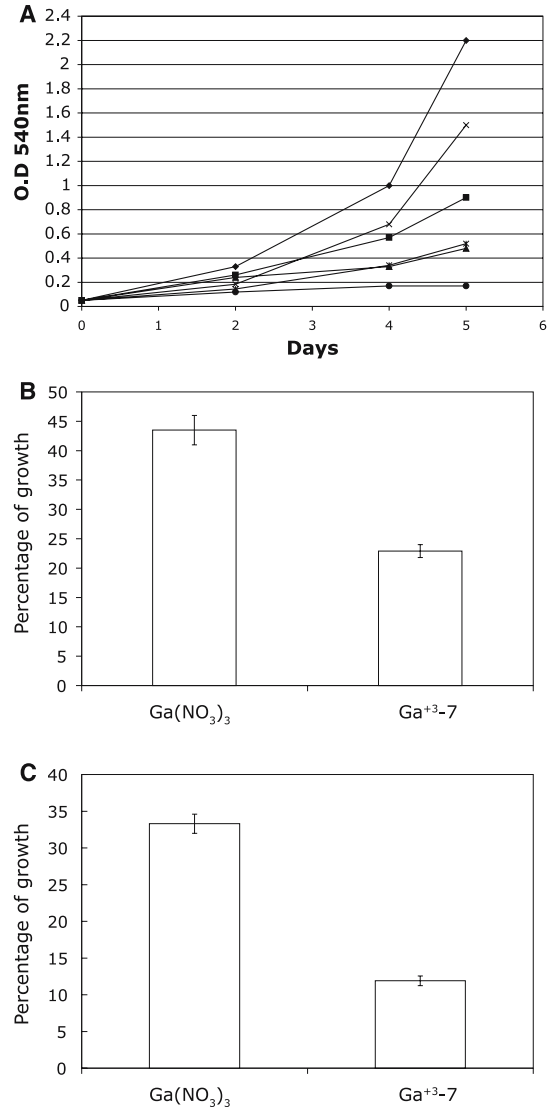

Fig. 7 (**A**) Growth of H37Rv and ST73 in the presence of Ga. H37Rv in MM (♦), H37Rv in MM with 50 μM $[Ga(NO_3)_3]$ (■), H37Rv in MM with 50 μM of Ga^{3+}-**7** (▲), ST73 in MM with 2 μM of $FeCl_3$ (×), ST73 in MM with 2 μM of $FeCl_3$ and 50 μM $[Ga(NO_3)_3]$ (*), ST73 in MM with 2 μM of $FeCl_3$ and 50 μM of Ga^{3+}-**7** (•). The results of one representative experiment are shown. The experiment was repeated three times. Growth of H37Rv (**B**) and ST73 (**C**) after 5 days of incubation in the presence of $[Ga(NO_3)_3]$ and Ga^{3+}-**7** expressed as percentage of growth relative to the control culture with no Ga(III) added

In summary, *M. tuberculosis* has the capacity to utilize the synthetic siderophore derivatives of acinetoferrin (**5-8**) but not all citrate-based siderophores (e.g., petrobactin **9**). Growth promotion experiments using mutant strains revealed two pathways for the utilization of the cyclic acinetoferrin derivatives. The first was a low-affinity, native-siderophore-independent pathway and the second was more efficient and probably involves transfer of the metal (iron or gallium) to mycobactin. Certain structural motifs seem preferred. In particular, an imide group was identified as a molecular feature for superior iron delivery activity into *M. tuberculosis*. This finding suggested that specific molecular recognition events were involved. Siderophores (**7** and **8**) with clogP values near 7 were shown to be better growth stimulants, which suggested that lipophilicity may play a role in delivery of iron to *M. tuberculosis* via xenosiderophores.

The ability to access mycobactin is therefore an important feature that enhances metal delivery and it can be exploited, as shown here, to deliver toxic metal ions such as gallium (III). As demonstrated in this study, synthetic siderophores like **7** and **8** are useful probes to learn about iron transport in *M. tuberculosis*. Further characterization of the molecular and structural requirements for iron delivery can facilitate the future development of inhibitors of siderophore biosynthesis (Ferreras et al. 2005; Somu et al. 2006), inhibitors of iron transport and ''Trojan horses'' that carry antimicrobials into this pathogen (Miller and Malouin 1993). The cytotoxic action of the gallium complex of **7** represents a new illustration of the latter antimicrobial delivery concept in action.

Acknowledgements The studies were supported by NIH research grant RO1 A1 44856 (awarded to Issar Smith). The authors thank Jodie Johnson at the University of Florida mass spectrometry facility for performing the LC-MS analysis. We thank Issar Smith for his support, helpful discussions and critical reading of the manuscript.

References

Anderegg G, L'Eplattenier F, Schwarzenbach G (1963) Hydroxamate complexes. III. Iron(III) exchange between sideramides and complexones. A discussiion of the formation constants of the hydroxamate complexes. Helv Chim Acta 46:1409

Barbeau K, Zhang G, Live DH, Butler A (2002) Petrobactin, a photoreactive siderophore produced by the oil-degrading marine bacterium *Marinobacter hydrocarbonoclasticus*. J Am Chem Soc 124:378–379

Bergeron RJ, Huang G, Smith RE, Neelam B, McManis JS, Butler A (2003) Total synthesis and structure revision of petrobactin. Tetrahedron 59:2007–2014

Braun V, Killmann H (1999) Bacterial solutions to the iron-supply problem. TIBS 24:104–109

Budzikiewicz H (2004) Siderophores of the *Pseudomonadaceas sensu stricto* (fluorescent and non-fluorescent *Pseudomonas* spp.). In: Herz W, Falk H, Kirby GW (eds) Progress in chemistry of organic natural products, vol 87. springer-Verlag, New York, 176 pp

De Voss JJ, Rutter K, Schroeder BG, Su H, Zhu Y, Barry CE III (2000) The salicylate-derived mycobactin siderophores of *Mycobacterium tuberculosis* are essential for growth in macrophages. Proc Natl Acad Sci 97:1252–1257

DeAngelis CD, Flanigan A (2005) Tuberculosis – a global problem requiring a global solution. JAMA 293:2793–2794

Ferreras JA, Ryu JS, Di Lello F, Tan DS, Quadri LEN (2005) Small-molecule inhibition of siderophore biosynthesis in *Mycobacterium tuberculosis* and *Yersinia pestis*. Nat Chem Biol 1:29–32

Gardner RA, Ghobrial G, Naser SA, Phanstiel O IV (2004a) Synthesis and biological evaluation of new Acinetoferrin homologues for use as iron transport probes in mycobacteria. J Med Chem 47:4933–4940

Gardner RA, Kinkade R, Wang C, Phanstiel O IV (2004b) Total synthesis of petrobactin and its homologues as potential growth stimuli for *Marinobacter hydrocarbonoclasticus*, an oil-degrading bacteria. J Org Chem 69:3530–3537

Girijavallabhan V, Miller MJ (2004) Therapeutic uses of Iron(III) chelators and their antimicrobial conjugates. In: Crosa JH, Mey AR, Payne SM (eds) Iron transport in bacteria. ASM Press, Washington, DC, pp 413–433

Gobin J, Moore CH, Reeve JRJ, Wong DK, Gibson BW, Horwitz MA (1995) Iron acquisition by *Mycobacterium tuberculosis*: isolation and characterization of a family of iron-binding exochelins. Proc Natl Acad Sci USA 92:5189–5193

Gobin J, Horwitz M (1996) Exochelins of *Mycobacterium tuberculosis* remove iron from human iron-binding proteins and donate iron to mycobactins in the *M. tuberculosis* cell wall. J Exp Med 183:1527–1532

Guo H, Naser SA, Ghobrial G, Phanstiel O IV (2002) Synthesis and biological evaluation of new citrate-based siderophores as potential probes for the mechanism of iron uptake in mycobacteria. J Med Chem 45:2056–2063

Harris WR, Carrano CJ, Cooper SR, Sofen SR, AVdeef AE, McArdle JV, Raymond KN (1979) coordination chemistry of microbial iron transport compounds. 19. Stability constants and electrochemical behavior of ferric enterobactin and model complexes. J Am Chem Soc 101:6097

Hawkes GE, O'Brien P, Salacinski H, Motevalli M, Abrahams I (2001) Solid and solution state NMR spectra and the structure of the Gallium Citrate complex $(NH_4)_3[Ga(C_6H_5O_7)_2]4H_2O$. Eur J Inorg Chem 2001:1005–1011

Heggemann S, Schnabelrauch M, Klemm D, Mollmann U, Reissbrodt R, Heinisch L (2001) New artificial siderophores based on a monosaccharide scaffold. BioMetals 14:1–11

Jarlier V, Nikaido H (1994) Mycobacterial cell wall: structure and role in natural resistance to antibiotics. FEMS Microbiol Lett 123:11–18

Koppisch A, Browder C, Moe A, Shelley J, Kinkel B, Hersman L, Iyer S, Ruggiero C (2005) Petrobactin is the primary siderophore synthesized by *Bacillus anthracis* str. Sterne under conditions of iron starvation. BioMetals 18:577–585

Lin YM, Miller MJ, Mollmann U (2001) The remarkable hydrophobic effect of a fatty acid side chain on the microbial growth promoting activity of a synthetic siderophore. BioMetals 14:153–157

Loper JE, Henkels MD (1999) Utilization of heterologous siderophores enhances levels of iron available to *Pseudomona putida* in the rhizosphere. Appl Environ Microbiol 65:5357–5363

Luo M, Lin H, Fischbach MA, Liu DR, Wailsh CT, Groves JT (2006) Enzymatic tailoring of enterobactin alters membrane partitioning and iron acquisition. ACS Chem Biol 1:29–32

Matzanke BF, Bohnke R, Mollmann U, Reissbrodt R, Schunemann V, Tratwein AX (1997) Iron uptake and intracellular metal transfer in mycobacteria mediated by xenosiderophores. BioMetals 10:193–203

Matzapetakis M, Raptopoulou CP, Tsohos A, Papaefthymiou V, Moon N, Salifoglou A (1998) Synthesis,spectroscopic and structural characterization of the first mononuclear, water soluble iron-citrate complex $(NH_4)_5Fe(C_6H_4O_7)_2$ $2H_2O$. J Am Chem Soc 120:13266–13267

Miller MJ, Malouin F (1993) Microbial iron chelators as drug delivery agents: the rational design and synthesis of siderophore-drug conjugates. Acc Chem Res 26:241–249

Olakanmi O, Britigan BE, Schlesinger LS (2000) Gallium disrupts iron metabolism of mycobacteria residing within human macrophages. Infect Immun 68:5619–5627

Payne SM, Mey AR (2004) Iron transport in pathogenic *Escherichia coli*, *Shigella* and *Salmonella*. In: Crosa JH, Mey AR, Payne SM (eds) Iron transport in bacteria. ASM Press, Washington, pp 199–219

Ratledge C, Patel PV, Mundy J (1982) Iron transport in *Mycobacterium smegmatis*: the location of mycobactin by electron microscopy. J Gen Microbiol 128:1559–1565

Ratledge C, Dover LG (2000) Iron metabolism in pathogenic bacteria. Annu Rev Microbiol 54:881–941

Reissbrodt R, Ramiandrasoa F, Bricard L, Kunesch G (1997) Siderophore activity of chemically synthesized dihydroxybenzoyl derivatives of spermidines and cystamide. BioMetals 10:95–103

Rodriguez GM, Voskuil MI, Gold B, Schoolnik GK, Smith I (2002) *ideR*, An essential gene in *Mycobacterium tuberculosis*: role of IdeR in iron-dependent gene expression, iron metabolism, and oxidative stress response. Infect Immun 70:3371–3381

Rodriguez GM, Smith I (2006) Identification of an ABC transporter required for iron acquisition and virulence in *Mycobacterium tuberculosis*. J Bacteriol 188:424–430

Roosenberg JMI, Lin YM, Lu Y, Miller MJ (2000) Studies and synthesis of siderophores, microbial iron chelators, and analogs as potential drug delivery agents. Curr Med Chem 7:159–197

Schumann G, Mollmann U (2001) Screening system for xenosiderophores as potential drug delivery agents in mycobacteria. Antimicrob Agents Chemother 45:1317–1322

Schwyn B, Neilands JB (1987) Universal chemical assay for the detection and determination of siderophores. Anal Biochem 160:47–56

Somu RV, Boshoff H, Qiao C, Bennett EM, Barry CE 3rd, Aldrich CC (2006) Rationally designed nucleoside antibiotics that inhibit siderophore biosynthesis of *Mycobacterium tuberculosis*. J Med Chem 49:31–34

Wang QX, Phanstiel O IV (1998) Total synthesis of acinetoferrin. J Org Chem 63:1491–1495

Weinberg ED (1984) Iron withholding: a defense against infection and neoplasia. Physiol Rev 64:65–102

Winkelmann G (1991) Handbook of microbial iron chelates. CRC, Boca Raton FL

Wittmann S, Heinisch L, Scherlitz-Hofmann I, Stoiber T, Ankel-Fuchs D, Mollmann U (2004) Catecholates and mixed catecholate hydroxamates as artifcial siderophores for mycobacteria. BioMetals 17:53–64

Xu Y, Miller MJ (1998) Total syntheses of mycobactin analogues as potent antimicobacterial agents using a minimal protecting group strategy. J Org Chem 63:4314–4322